PROCEEDINGS OF SCIENCE

Exploring multi-pulse GRB prompt emission via novel pulse shape model

Gowri A,[a,*] **Asaf Pe'er,**[b] **Felix Ryde**[c] **and Hüsne Dereli-Bégué**[b]

[a] *Indian Institute of Science Education and Research, Mohali, India*

[b] *Bar Ilan University, Ramat Gan, Israel*

[c] *KTH, Stockholm, Sweden*

E-mail: gowri.a.99@gmail.com

The light curves of the prompt phase of gamma-ray bursts (GRBs) exhibit erratic and diverse behaviour, often with multiple pulses. The temporal shape of individual pulses is often modelled as 'fast rise exponential decay' (FRED). Here, we propose a novel fitting function to measure pulse asymmetry. We perform a time-resolved spectrum analysis on a sample of 75 pulses from twenty-seven GRBs that the *Fermi* Gamma-ray Burst Monitor has identified. When multi-pulse bursts are taken into account, a distinct behaviour becomes evident: the first pulses have the most symmetric-like lightcurve, while subsequent pulses show an increase in the asymmetry parameter, leading to a more FRED-like form. Furthermore, we correlate pulse temporal and spectral shapes after fitting the spectra with the classical "Band" function. A moderate positive Spearman correlation between pulse asymmetry and the low-energy spectral index α_{max} (where the maximum is taken over all time bins that cover the pulse shape) is identified. An overlapping emission mechanism is indicated by the fact that $\sim 64\%$ of the GRB pulses fall within the limits of the slow-cooling synchrotron and non-dissipative photospheric emission models. Thus, our findings offer a compelling hint towards understanding the origin of GRB pulses.

High Energy Phenomena in Relativistic Outflows (HEPRO) - VIII,
23-26 October 2023
Institut d'Astrophysique de Paris and Observatoire de Paris, Paris, France

*Speaker

© Copyright owned by the author(s) under the terms of the Creative Commons Attribution-NonCommercial-NoDerivatives 4.0 International License (CC BY-NC-ND 4.0).

PoS(HEPROVIII)054

1. Introduction

Gamma Ray Bursts (GRBs) are intense bursts of gamma rays lasting seconds to hundreds of seconds, exhibiting diverse behaviours in prompt light curves, including multiple pulses. A comprehensive model necessitates understanding the origins of individual pulse characteristics, including duration, shape, spectrum, and their interrelations.
Early studies [1, 2] identified an asymmetric character in the pulse shapes - commonly Fast Rise Exponential Decay (FRED) shape, indicating rapid energy release and dissipation. However, our visual survey revealed instances of temporal symmetry in some pulses, contrary to the established asymmetric nature of single pulses. In our investigation, we focused on studying the pulse shapes and discerning the patterns in these shapes to provide new insight into underlying radiative emission mechanisms and jet dynamics. Employing a novel pulse shape function on multipulse GRB data obtained by *Fermi* Gamma-Ray Burst Monitor (GBM), our investigation aims to elucidate how pulse shapes, and consequently emission mechanisms within bursts, evolve over time.
Spectral analysis of photon energy distributions is a primary method for investigating GRB emission mechanisms. In the Fireball model, prompt emission arises from energy dissipation within a highly relativistic jet ejected during black hole formation [3, 4]. Two prominent emission mechanisms, assuming leptonic origin, are proposed. The first involves radiation from the photosphere region, where the jet becomes transparent [5, 6]. Alternatively, photons may originate from regions farther from the progenitor, following jet kinetic or magnetic energy dissipation. This energy dissipation accelerates electrons to emit synchrotron radiation [7–9], potentially accompanied by inverse Compton scattering at high energies. The low-energy spectral index (α) serves as a proxy for the emission mechanism. The synchrotron emission is indicated by the limits, $\alpha \leq -0.66$, while $\alpha \geq +0.4$ suggests a non-dissipative photospheric origin. We further explore the correlation between the pulse shapes and spectral shapes to understand the underlying emission mechanism.

2. Data Analysis

The “pulses", considered to be the fundamental emission units in the prompt phase, are identified in the GRB data obtained by the *Fermi* - GBM, covering an energy range of 8 keV to 40 MeV across 12 NaI and 2 BGO detectors. Each pulse in a lightcurve adheres to specific criteria: it starts from a background level or immediately follows another pulse, with the start of the rising phase defined when the count rate is at most 50-55% of the peak count rate. Similarly, the end of the decay phase returns to background levels, or if overlapping, ends when the count rate is at most 50-55% of the peak, followed by another pulse.

We also require that each pulse have at least two Bayesian time bins, with a statistical significance $S \geq 20$, representing the signal-to-noise ratio [10]. Additionally, selected pulses must maintain the coefficient of determination $r^2 \geq 0.7$ after fitting with the novel function. We have chosen a sample set of 27 GRBs consisting of 75 pulses that follow our selection criteria.

2.1 Pulse shape analysis

Equation 1 provides an approximate sigmoid function with 5 degrees of freedom that is versatile enough to fit both FRED and symmetric pulse shapes due to its flexible parameters.

PoS(HEPROVIII)054

The empirical pulse model function labelled as peer_ag is given by,

$$I(t) = A \times \left[1 - \tanh\left(\frac{1}{s_r}(t - r_r)\right)\right] \times \left[1 + \tanh\left(\frac{1}{s_l}(t - r_l)\right)\right]. \quad (1)$$

Here, I(t) is given in units of counts/s, s_l and s_r represent the rising (left) and decaying (right) slopes of the lightcurve - larger values imply steeper slopes (on the left and right side, respectively). The parameters r_l and r_r denote the time for the lightcurve to rise and fall by half, respectively, and A is a global normalization. This function is suitable for analyzing single-peaked sections of the light curve, being sensitive to fluctuations within a pulse. Pulses exhibiting multiple smaller peaks and variations are classified as combined peak pulses.
We define the **pulse shape parameter** as the ratio between the rising and decaying slopes,

$$\text{pulse shape} = \frac{s_l}{s_r}. \quad (2)$$

Asymmetry in the pulse shape can be quantified using this ratio. Some example fits are given in Figure 1.

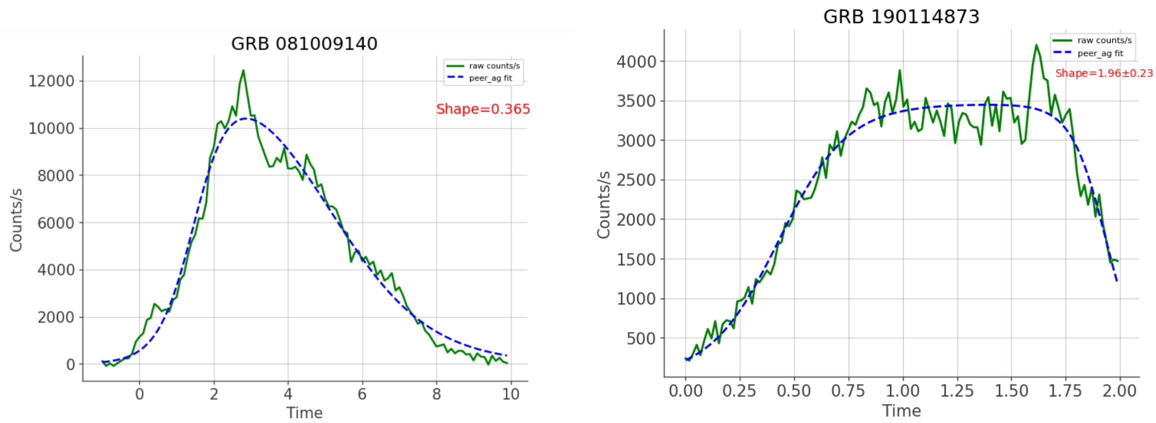

Figure 1: Example fit for a pulse in GRB 081009 with our function. Here, the shape parameter = 0.36, and the pulse is **FRED-like.** Example fit for a pulse in GRB 190114 with our function. Here the shape parameter = 1.96, and the pulse is **Symmetric-like.**

2.2 Spectral analysis

GRB spectral analysis entails fitting spectra using an empirical model, with α_{max} as a crucial indicator of the radiative mechanism, analyzed through the Bayesian tool 3ML [11]. For a time-resolved spectral analysis, Bayesian block binning identifies constant Poisson rate intervals, and the data is rebinned to minimize the variations in emission. The spectral parameters are well-constrained for at least two bins with $S \geq 20$. Consistent binning is extended to other detectors.

The Band function spectral fit [12] was utilized to model the pulse spectra, providing a better fit for the pulses obtained from [13]. Each time bin in the pulse can have a different low energy spectral index α. However, each physical emission model imposes constraints on the maximum α value. Assuming a singular emission mechanism, we adopted the methodology from the previous studies [14–16], selecting the bin with the highest α—referred to as α_{max}—for subsequent analysis.

PoS(HEPROVIII)054

3. Results

Following section 2, we calculate the pulse shapes as defined in Equation 2 above, pulse number, i.e. the corresponding order of each pulse in a burst (1^{st}, 2^{nd} etc.), and the α_{max} values. We denoted the pulses with shape ≤ 0.3 as FRED-like and shape ≥ 0.7 as symmetric-like.

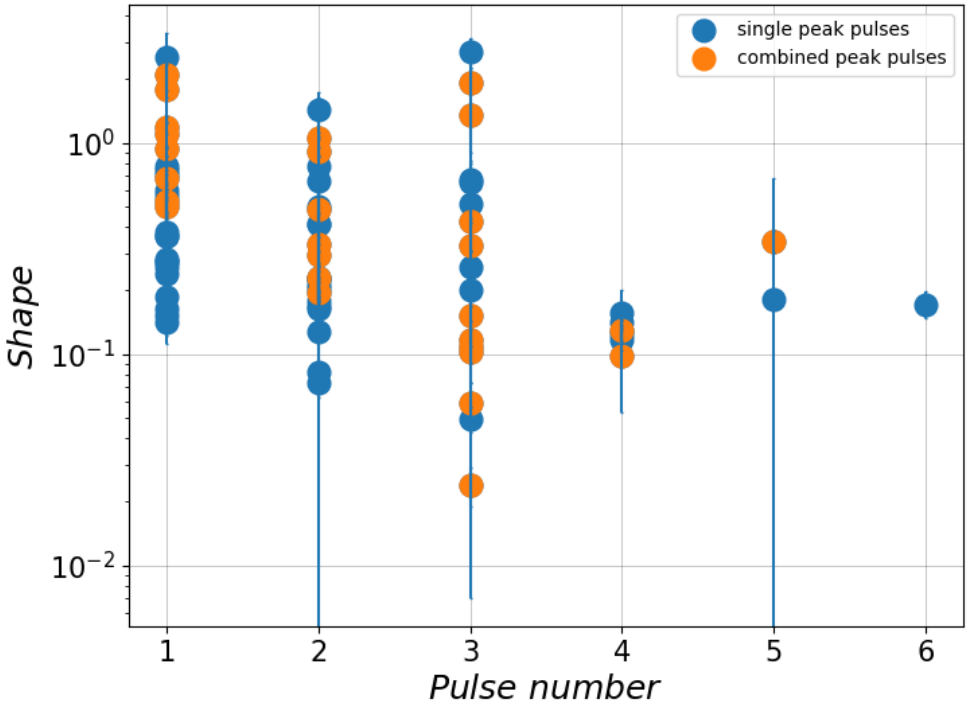

Figure 2: The pulse shape - pulse number relation. The blue and orange dots present the single and combined pulses, respectively. Errors are in one σ significance.

In Figure 2, we plot the shape of each of the 75 pulses in our sample as a function of the pulse number, and the results follow as below. Firstly, the pulse shape largely changes over time with the pulse number. The temporal pulse shape changes from symmetric-like to FRED-like as the burst evolves, with Spearman's rank correlation coefficient $r_s = -0.41$, p-value = 0.0002. This indicates a mild anti-correlation between the pulse shape and pulse number. Secondly, we find that $16/75 \sim 21\%$ of the pulses have a symmetric-like shape, and $39/75 \sim 52\%$ of the pulses fall in between a FRED-like and symmetric-like shape. We also note that $13/49 \sim 26\%$ of the first pulses have shape function ≥ 0.7, indicating that they are nearly symmetric. However, the picture changes when looking at later (3rd onward) pulses: only $3/26 \sim 11\%$ have shape ≥ 0.7.

From Figure 3, of the spectral shape α_{max} values of each pulse as a function of the pulse shape plot, we analyse the effect on the emission mechanism by the pulse shape. We notice a mild correlation from Spearman's correlation coefficient $r_s = 0.35$ with a p-value = 0.002. Here, the symmetric-like pulses have harder α_{max} values than FRED-like pulses. Notably, all pulses have α_{max} values above the theoretical prediction limit of $\alpha_{max} \leq -1.5$ in the "fast cooling" synchrotron emission model (Purple line in Figure 3), indicating incompatibility with efficient electron cooling in the jet. But 64% of the pulses are between the NDP line and the slow cooling synchrotron line, showing a bias towards thermal overlap in the emission, whereas 35% are between the slow cooling

PoS(HEPROVIII)054

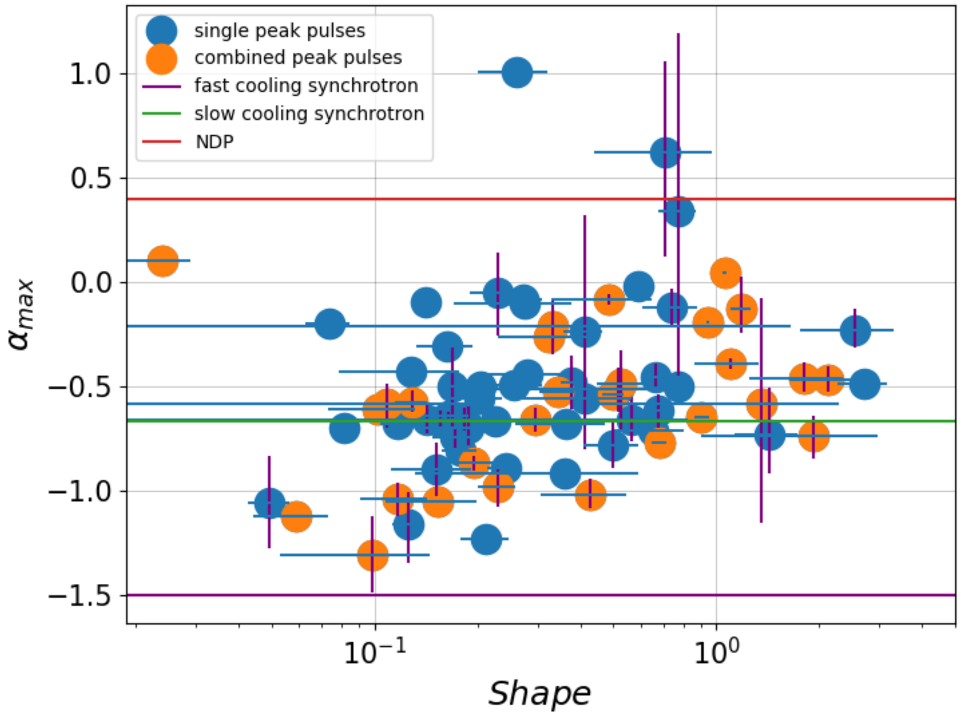

Figure 3: The α_{max} - pulse shape relation. The blue and orange data points are single-peak pulses and combined-peak pulses. The green, red and purple lines represent the upper limits for the fast and slow cooling synchrotron and the theoretical non-dissipative photospheric (NDP) emission, respectively.

synchrotron and fast cooling synchrotron lines, showing dominant non-thermal emission origins. These results are now in the final stages of preparation for publication (Gowri et al. 2024 in prep).

4. Conclusions

Our investigation into the discernible patterns in pulse shapes of GRBs combined with the spectral analysis provides unique insights into the radiative mechanism and jet dynamics involved in the prompt phase. From our pulse shape studies in Figure 2, we conclude that our novel pulse shape function is able to quantify the symmetry in pulse shapes. This means rise and decay timescales are similar in these pulses. The photospheric emission may explain this, as the photons that are emitted below the photosphere diffuse through the plasma until they escape, causing a more symmetric pulse structure.

It is also clear that initial pulses are more symmetric-like, and later pulses are more FRED-like. From our spectral shape-pulse shape studies in Figure 3, we note that the symmetric-like pulses tend to have harder α_{max} values than the FRED-like pulses. This indicates that the emission mechanism at different radii of the jet is likely changing throughout the burst from thermal to non-thermal.

References

[1] J.P. Norris, J.T. Bonnell, R.J. Nemiroff, J.D. Scargle, G.N. Pendleton, C. Kouveliotou et al., *Time Dilation and Homogeneous, Soft-Spectrum GRBs*, .

PoS(HEPROVIII)054

[2] J. Hakkila and R.D. Preece, *Unification of Pulses in Long and Short Gamma-Ray Bursts: Evidence From Pulse Properties and Their Correlations*, *The Astrophysical Journal* **740** (2011) 104.

[3] M.J. Rees and P. Meszaros, *Relativistic fireballs - Energy conversion and time-scales.*, *Monthly Notices of the Royal Astronomical Society* **258** (1992) 41.

[4] P. Mészáros, E. Ramirez-Ruiz, M.J. Rees and B. Zhang, *X-Ray-rich Gamma-Ray Bursts, Photospheres, and Variability*, *The Astrophysical Journal* **578** (2002) 812.

[5] M.J. Rees and P. Mészáros, *Dissipative Photosphere Models of Gamma-Ray Bursts and X-Ray Flashes*, *The Astrophysical Journal* **628** (2005) 847.

[6] A. Pe'er, P. Mészáros and M.J. Rees, *Radiation from an Expanding Cocoon as an Explanation of the Steep Decay Observed in GRB Early Afterglow Light Curves*, *The Astrophysical Journal* **652** (2006) 482.

[7] T. Piran, A. Shemi and R. Narayan, *Hydrodynamics of Relativistic Fireballs*, *Monthly Notices of the Royal Astronomical Society* **263** (1993) 861.

[8] R. Sari, T. Piran and R. Narayan, *Spectra and Light Curves of Gamma-Ray Burst Afterglows*, *The Astrophysical Journal* **497** (1998) L17.

[9] N.M. Lloyd and V. Petrosian, *Synchrotron Radiation as the Source of Gamma-Ray Burst Spectra*, *The Astrophysical Journal* **543** (2000) 722.

[10] G. Vianello, *The Significance of an Excess in a Counting Experiment: Assessing the Impact of Systematic Uncertainties and the Case with a Gaussian Background*, **236** (2018) 17 [1712.00118].

[11] G. Vianello, R.J. Lauer, P. Younk, L. Tibaldo, J.M. Burgess, H. Ayala et al., *The Multi-Mission Maximum Likelihood framework (3ML)*, July, 2015. 10.48550/arXiv.1507.08343.

[12] D. Band, J. Matteson, L. Ford, B. Schaefer, D. Palmer, B. Teegarden et al., *BATSE Observations of Gamma-Ray Burst Spectra. I. Spectral Diversity*, **413** (1993) 281.

[13] L. Li, F. Ryde, A. Pe'er, H.-F. Yu and Z. Acuner, *Bayesian Time-resolved Spectroscopy of Multipulse GRBs: Variations of Emission Properties among Pulses*, *The Astrophysical Journal Supplement Series* **254** (2021) 35.

[14] H.-F. Yu, H. Dereli-Bégué and F. Ryde, *Bayesian Time-resolved Spectroscopy of GRB Pulses*, *The Astrophysical Journal* **886** (2019) 20.

[15] Z. Acuner, F. Ryde and H.-F. Yu, *Non-dissipative photospheres in GRBs: spectral appearance in the Fermi/GBM catalogue*, *Monthly Notices of the Royal Astronomical Society* **487** (2019) 5508.

[16] H. Dereli-Bégué, A. Pe'er and F. Ryde, *Classification of Photospheric Emission in Short GRBs*, **897** (2020) 145 [2002.06408].

PoS(HEPROVIII)054